Journal of Materials Chemistry B

Accepted Manuscript

This article can be cited before page numbers have been issued, to do this please use: M. H. Stenzel, M. Callari and D. S. Thomas, *J. Mater. Chem. B*, 2016, DOI: 10.1039/C5TB02429C.

ROYAL SOCIETY OF CHEMISTRY

www.rsc.org/materialsB

View Article Online
DOI: 10.1039/C5TB02429C

Journal Name

ARTICLE

The dual-role of Pt(IV) complexes as active drug and crosslinker for micelles based on β-cyclodextrin grafted polymer

Received 00th January 20xx,
Accepted 00th January 20xx

DOI: 10.1039/x0xx00000x

www.rsc.org/

Manuela Callari,[1] Donald S. Thomas,[2] Martina H. Stenzel[1]*

With a combination of RAFT and click chemistry an amphiphilic block copolymer with poly (ethylene glycol) methyl ether methacrylate (POEGMEMA) as hydrophilic block and poly (propargyl methacrylate) (PMA) as hydrophobic block has been successfully synthesized. To this, 6-azide-6-deoxy-β-cyclodextrin (N3-β-CD) was clicked creating a hosting environment for a hydrophobic small molecule platinum pro-drug. Oxoplatin, the oxidized version of cisplatin, has been modified on its axial ligand introducing cholic acid groups through esterification. This modified cisplatin forms a host-guest complex with β-cyclodextrin that has been characterised via NMR spectroscopy. The host-guest interaction that the drug established with the β-cyclodextrin grafted copolymer drove the self-assembly into nanoparticles of a diameter of 266 nm able to physical encapsulate the platinum-based drug. In the presence of ascorbic acid, 70% of the pro-drug is released over a period of 24 h. Cytotoxicity assays on ovarian cancer cells show that the polymer carrier improves the cytotoxicity of the platinum pro-drug. The IC50 value decreases from 37.7 μM with the pro-drug to 20.4 μM when the pro-drug is encapsulated into the polymer carrier. This is due to the fact that the uptake of the polymer carrier is up to 6 fold higher than the significantly smaller pro-drug by itself.

Introduction

Platinum based anti-cancer drugs have been used in clinic for decades, however, to date, there are many limitations.[1, 2] Platinum drugs are generally hydrophobic making their administration challenging and they are highly toxic causing a number of side effects.[3] In order to increase their solubility and reduce their toxicity different types of vehicles have been created to carry and deliver platinum drugs.[4] Among these, polymer nanoparticles (NPs) have been widely employed.[5] Polymer NPs show several advantages compared to the small drugs. They increase the circulation time and prevent fast clearance via the kidney thus reducing the administration dose. They can also exert an enhanced permeation and retention (EPR) effect in solid tumours.[6]

Platinum drugs can be either physically encapsulated or chemically bound to the polymer that forms the NP.[7, 8] The chemical conjugation of the platinum drug to the polymer backbone usually allows more efficient loading. However, the drug has to be cleavable from the polymer to be released from the NPs into the target.[9] When using physical encapsulation the release of the drug from the NPs is easier but stability and efficient loading can be a challenge.[10, 11] For these reasons, host-guest interactions between the drug and polymer moieties can be used to increase the loading efficiency and improve the stability of NPs. Ideal candidates to form host-guest complexes with hydrophobic drugs are cyclodextrins. In fact, their water solubility combined with their hydrophobic cavity makes them perfect holders for hydrophobic molecules.[12] Cyclodextrin (CD) alone has been conjugated to platinum drugs obtaining pro-drugs which can further encapsulate a second hydrophobic drug such as doxorubicin to give a dual-drug system able to enhance the anti-tumour activity.[13, 14] Up to date, there are no examples in literature of encapsulation of platinum drugs into cyclodextrins. However, it has been shown that chelating platinum drugs are able to form host-guest complexes with cyclodextrins.[15] A way researchers have found to establish an interaction between platinum drugs and cyclodextrins is to conjugate the drug to a moiety, such as adamantine, which can form host-guest complexes with cyclodextrins.[16, 17] Although cyclodextrins can enhance water solubility, due to their small size they cannot display the EPR effect to the same extent NPs can.[6] However, cyclodextrins can easily be clicked onto block copolymers and strengthen the interactions which allow the physical encapsulation of the drug.[18, 19] Cyclodextrin grafted block copolymers have been previously used to physically encapsulate hydrophobic anti-cancer drugs such as albendazole.[20] Next to its role as drug carrier, CD can be employed as a building block to generate complex polymer architectures,[21, 22] hydrogels,[23, 24] nanoparticles[25, 26] and crosslinked micelles.[27]

In this work, we investigate the use of CD as an anchor point to crosslink micelles while the Pt-containing crosslinker acts simultaneously as anti-cancer drug. Crosslinking of micelles has been shown to have a range of benefits including enhanced cellular uptake[28] and prolonged circulation in the blood stream.[29, 30]

[a] Centre for Advanced Macromolecular Design. School of Chemistry, University of New South Wales, Sydney NSW 2052, Australia *Email - M.Stenzel@unsw.edu.au
[b] Mark Wainwright Analytical Centre, University of New South Wales, Sydney NSW 2052, Australia

† Footnotes relating to the title and/or authors should appear here.
Electronic Supplementary Information (ESI) available: [detailed NMR investigations of the complex formation]. See DOI: 10.1039/x0xx00000x

View Article Online
DOI: 10.1039/C5TB02429C

However, permanent crosslinking can result in the accumulation of nanoparticles in the organs of the reticuloendothelial system (RES)[31, 32] and it is therefore desirable to introduce functional groups that can be cleaved once the drug has been released. A range of approaches are indeed available that allow the degradation of crosslinking units of the micelle.[33, 34] The pathway chosen here is to introduce a Pt(IV) pro-drug based on bile acid as axial ligand. Bile acid is known to form a host-guest complex with β-cyclodextrin,[35] but it is also known to be a cholesterol metabolite that is produced in the liver.[36] Block copolymers with pendant β-cyclodextrin groups are therefore synthesized by a combination of RAFT polymerization and click chemistry. The resulting water-soluble polymer will undergo self-assembly once the host-guest complexation with the hydrophobic bile acid-based Pt(IV) drug takes place (Scheme 1).

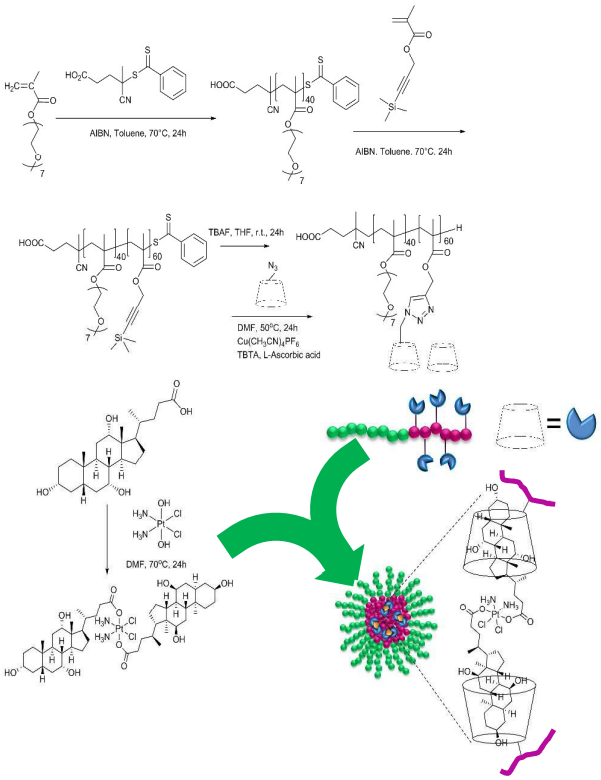

Scheme 1. Synthesis of block copolymer and Pt-drug cross-linker

Experimental section

Materials

The following chemicals were used as received from the supplier unless stated otherwise. Sodium azide (NaN_3, Sigma-Aldrich, 99%), 3-(trimethylsilyl)-2-propyn-1-ol (99%, Alfa Aesar), methacryloyl chloride (97%, Fluka), triethylamine (Et_3N, 99.5%, Sigma-Aldrich), tetra-*n*-butyl ammonium fluoride (TBAF, 1 M solution in THF, Sigma), acetic acid (99.8%, AR), cisplatin (99.9%, Sigma), 2,2'-Azobisisobutyronitrile (AIBN) was recrystallized from methanol prior to use, (Ethylene glycol methyl ether) methacrylate oligomer (OEGMEMA, AR) (M_n = 300 g/mol, Aldrich) was deinhibited before use by passing over basic alumina. The RAFT agent, 4-Cyanopentanoic Acid Dithiobenzoate (CPADB) was synthesised according to literature procedures,[37, 38] p-toluenesulfonyl chloride (99%, Sigma), Tris[(1-benzyl-1H-1,2,3-triazol-4-yl)methyl]amine (TBTA) (97%, Sigma), L-ascorbic acid (reagent grade, Sigma), tetrakis(acetonitrile)copper(I) hexafluorophosphate (97%, Sigma), cholic acid (from ox or sheep bile, 98%, Sigma), 4-(dimethylamino)pyridine (99%, Sigma), methyl-β-cyclodextrin (BioReagent, Sigma), β-cyclodextrin (Chem-Impex int'l inc.), N,N'-diisopropylcarbodiimide (DIC) (99%, Sigma)

Synthesis and procedures

Synthesis of $POEGMEMA_{40}$. Oligo(ethylene glycol methyl ether) methacrylate (OEGMEMA) (2 g, 6.66 mmol), 4-cyanopentanoic acid-4-dithiobenzoate (CPADB) (30 mg, 0.11 mmol) and AIBN (1.8 mg, 0.011 mmol) were dissolved in 7 ml of toluene in a Schlenk tube to give [OEGMEMA]/[CPADB]/[AIBN] = 60:1:0.1 ratio. The Schlenk tube was sealed and degassed using 3 freeze-pump-thaw cycles and leaving the reaction mixture under N_2. The reaction was stirred at 60 °C for 12 h. The reaction was quenched by dropping the tube into an ice bath and exposing the mixture to air. The polymer was precipitated twice in petroleum spirit and dried under vacuum at 40 °C overnight. ^{1}H NMR (300 MHz, $CDCl_3$, 25 °C): δ (ppm) = 7.90–7.15 (aromatic ring of CPDAB), 4.08 (2nH, $CH_3OCH_2CH_2O$), 3.66–3.53 (4nH, OCH_2CH_2O), 3.37 (3nH, $CH_3OCH_2CH_2O$), 1.97–1.77 (3nH, CH_3 of the main chain), 1.09–0.76 (2nH, CH_2 of the main chain), n being the degree of polymerization (DPn) of POEGMEMA. (X_{NMR} = 67%, $M_{n,theo}$ = 12000 g mol^{-1}, $M_{n,SEC}$ = 13800 g mol^{-1}, Đ = 1.1).

Synthesis of TMSPMA. 3-(Trimethylsilyl) propargyl alcohol (5.00 g, 5.71 ml, 39.0 mmol) was dissolved in 50 ml diethyl ether and purged with N_2 for 10 min. Dry triethylamine (4.40 ml, 49.3 mmol) was added while stirring and the reaction mixture was purged with N_2 for further 10 min in an ice bath. Methacryloyl chloride (6.10 ml, 68.2 mmol) was added drop wise over 1 h into the reaction mixture with stirring. The reaction was brought to room temperature and left stirring overnight, followed by filtration and solution concentration. The obtained residue was purified via column chromatography taking petroleum ether: diethyl ether (50:1) as eluent and obtaining a very pale yellow oil (3.7 g, 74%). ^{1}H NMR (300 MHz, $CDCl_3$, 25 °C): δ (ppm) = 6.20-5.62 (4nH, $C=CH_2$), 4.36 (2nH, OCH_2C), 1.98 (3nH, CH_3), 0.15 (9nH, $Si(CH_3)_3$).

Synthesis of $POEGMEMA_{40}$-*b*-$TMSPMA_{60}$. The POEGMEMA macro-RAFT (0.5 g, 5.10 x 10^{-2} mmol), was dissolved together with 3-(Trimethylsilyl)-2-propyn-1-yl methacrylate (TMSPMA) (1 g, 5.10 mmol) and AIBN (0.83 mg, 5.10 x 10^{-3} mmol) in 4 ml of toluene in a Schlenk tube to give [POEGMEMA]/[TMSPMA]/[AIBN] = 1:100:0.1 ratio. The Schlenk tube was sealed and degassed using 3 freeze-pump-thaw cycles and leaving the reaction mixture under N_2. The reaction was let stir at 60 °C for 12 h. The reaction was quenched by exposing it to the air and dropping the temperature by placing the Schlenk tube into an ice bath. The polymer was precipitated twice

View Article Online
DOI: 10.1039/C5TB02429C

in petroleum spirit and dried under vacuum at 40 °C overnight. ^{1}H NMR (300 MHz, $CDCl_3$, 25 °C): δ (ppm) = 7.90−7.15 (aromatic ring of CPDAB), 4.59 (2mH, OCH_2C), 4.08 (2nH, OCH_2CH_2O), 3.80−3.48 (4nH, OCH_2CH_2O), 3.39 (3nH, $CH_3OCH_2CH_2O$), 1.97−1.77 (3n+mH, CH_3 of the main chain), 1.09−0.76 (2n+mH, CH_2 of the main chain), 0.15 (9nH, $Si(CH_3)_3$), n being the degree of polymerization (DPn) of POEGMEMA and m being the degree of polymerization (DPn) of TMSPMA. (X_{NMR} = 60%, $M_{n,theo}$ = 11760 g mol^{-1}, $M_{n,SEC}$ = 23800 g mol^{-1}, Đ = 1.20).

Deprotection POEGMEMA$_{40}$-*b*-TMSPMA$_{60}$. The trimethylsilyl protected block polymer (0.447 g, 1.85 x 10^{-2} mmol) was dissolved in THF (10 mL) and acetic acid (2 molar equivalent with respect to the alkyne-trimethylsilyl groups) in a round bottom flask. The flask was sealed and the solution was purged with N_2 for 20 min while stirring in an ice bath. A 1 M solution of TBAF·3H$_2$O in THF (2 molar equivalent with respect to the alkyne-trimethylsilyl groups) was slowly added with a syringe. The turbid mixture was let stir at 0 °C for 30 min, then at room temperature for 24 h. The reaction was passed through a short silica pad to remove the TBAF, concentrated under reduced pressure and diluted in chloroform. The deprotected polymer was precipitated in petroleum ether (40-60 °C) and dried under vacuum at 40 °C overnight. ^{1}H NMR (300 MHz, $CDCl_3$, 25 °C): δ (ppm) = 7.90−7.15 (aromatic ring of CPDAB), 4.59 (2mH, OCH_2C), 4.08 (2nH, OCH_2CH_2O), 3.80−3.48 (4nH, OCH_2CH_2O), 3.39 (3nH, $CH_3OCH_2CH_2O$), 2.55 (nH, CCH), 1.97−1.77 (3n+mH, CH_3 of the main chain), 1.09−0.76 (2n+mH, CH_2 of the main chain), n being the degree of polymerization (DPn) of POEGMEMA and m being the degree of polymerization (DPn) of TMSPMA. ($M_{n,theo}$ = 11760 g mol^{-1}, $M_{n,SEC}$ = 20000 g mol^{-1}, Đ = 1.28).

Synthesis of N$_3$-β-CD. The compound was synthesis using an established procedure.[39] β-CD (60.0 g, 52.9 x 10^{-3} mol) was suspended in 500 ml of water to which a solution of NaOH (6.57 g, 164.0 x 10^{-3} mol) in 20 ml of water was added drop wise over 6 min. The suspension became homogeneous and slightly yellow. p-Toluenesulfonyl chloride (10.08 g, 52.9 x 10^{-3} mol) dissolved in 30 ml of acetonitrile was then added causing immediate formation of a white precipitate. After 2 h of stirring at room temperature the precipitate was filtered and the solution concentrated. The white product was filtered and dried in a vacuum oven at 40 °C. (10 g, 7.8 x 10^{-3} mol, 14%). The tosylated β-CD (10 g, 7.7 x 10^{-3} mol) was suspended in dry DMF (1.5 ml), the mixture becomes homogeneous after warming up to 60 °C. Crystalline KI (0.63 g, 3.8 x 10^{-3} mol) and NaN_3, (5 g, 77 x 10^{-3} mol) were added to the mixture and let stirring at 60-65 °C for 24 h. The reaction was then cooled to room temperature, acetone (100 ml) was added to produce a white precipitate that was recovered by filtration and dried in vacuum oven at 40 °C. (3 g, 2.6 x 10^{-3} mol, 33%, total yield 5%). (ESI-MS Calcd *m/z* for $C_{42}H_{69}N_3O_{34}$, 1159.38; experimental *m/z*, 1157.5) (Fig. S1).

Synthesis of POEGMEMA$_{40}$-*b*-TMSPMA$_{60}$-*g*-βCD. POEGMEMA$_{40}$-*b*-PMA$_{60}$ (100 mg, 5.1 x 10^{-3} mmol) and N$_3$-β-CD (355 mg, 3.06 x 10^{-1} mmol) (1 eq. compare to the alkyne groups) were dissolved in DMF (2 ml). A solution of TBTA (17.8 mg, 3.36 x 10^{-2} mmol) and L-Ascorbic acid (53.8 mg, 3.06 x 10^{-2} mmol) in DMF (2 ml) was added to the N$_3$-β-CD solution while stirring and under a flow of N_2. The N_2 was purged for about 20 min and then $Cu(CH_3CN)_4PF_6$ (11.4 mg, 3.06 x 10^{-2} mmol) was added slowly. The reaction was stirred overnight at 50 °C. The product was dialysed against DMSO first and H_2O after, it was then freeze dried. The solid was redissolved in DMSO, mixed with a copper chelating resin and shaken for 24 h at 37 °C. The resin was then filtered out; the filtrate was dialysed against H_2O and freeze dried (380 mg, 80%). ^{1}H NMR (300 MHz, d_6-DMSO, 25 °C): δ (ppm) = 8.30−7.9 (triazole), 6.4-5.5, 5.3-4.7, 4.7-4.2 (H3, H6, H5, H3, H4), 4.1 (2nH, OCH_2CH_2O), 3.80−3.48 (4nH, OCH_2CH_2O), 3.5-2.7 (3nH, $CH_3OCH_2CH_2O$), 1.97−1.77 (3n+mH, CH_3 of the main chain), 1.09−0.76 (2n+mH, CH_2 of the main chain),

Synthesis of CA-Pt. Oxoplatin was prepared via oxidation of the commercially available cisplatin. Briefly, cisplatin is suspended in hydrogen peroxide solution (30% in water) and stirred at 75 °C for 5h and then overnight at room temperature. The mixture is then freeze dried giving a pale yellow powder. Oxoplatin (0.2 g, 2.99 x 10^{-4} mol) was dissolved in DMF (3 ml) in a round bottom flask which was sealed and purged with N_2. A solution of cholic acid (0.232 g, 5.68 x 10^{-4} mol) and DMAP (0.0365 g, 2.99 x 10^{-4} mol) in DMF was added to the oxoplatin solution while stirring. After few minutes of stirring, DIC (0.093 ml, 5.98 x 10^{-4} mol) was added. The reaction was stirred overnight at room temperature. The yellow suspension was filtered to remove the urea and then put under reduced pressure to remove the DIC. Lastly, the product was precipitated in water, filtered and freeze dried (0.258 g, 75%). ^{1}H NMR (300 MHz, $CDCl_3$, 25 °C): δ (ppm) = 3.77 (CH), 3.6 (CH), 3.17 (CH), 2.13 (CH), 2.09, 2.21 (CH_2), 1.97 (CH), 1.77 (CH), 1.45, 2.21 (CH_2), 1.36, 1.78 (CH_2), 1.35, 1.41 (CH_2), 1.32 (CH), 1.28 (CH), 1.26, 1.41 (CH_2), 1.22 (CH), 1.19, 1.64 (CH_2), 1.15, 1.71 (CH_2), 0.96, 1.63 (CH_2), 0.91 (CH_3), 0.83, 1.63 (CH_2), 0.8 (CH_3), 0.58 (CH_3)

Preparation of β-CD/CA-Pt complex. β-CD (99 mg, 8.72 x 10^{-5} mol) was dissolved in 6 ml of H_2O while CA-Pt (50 mg, 4.36 x 10^{-5} mol) was dissolved in 6 ml of THF. The THF solution was added drop wise to the H_2O solution. The solution turned turbid at first but turned clear after being stirred at high speed at 40 °C for 24 h. The THF was then evaporated slowly at 40 °C in an open vessel. The remaining solution was freeze dried.

Preparation of Me-β-CD/CA-Pt complex. Me-β-CD (70 mg, 5.34 x 10^{-5} mol) was dissolved in 3 ml of H_2O while CA-Pt (25 mg, 2.18 x 10^{-5} mol) was dissolved in 3.5 ml of THF. The THF solution was added drop wise to the H_2O solution while stirring. The mixture was stirred at high speed at 40 °C for 24 h. The THF was then evaporated slowly at 40 °C in an open vessel. The remaining solution was freeze dried.

Micelles preparation POEGMEMA$_{40}$-*b*-PMA$_{60}$-*g*-β-CD$_{(80\%)}$/CA-Pt. The polymer (11 mg, 9.82 x 10^{-8} mol) and the CA-Pt (4.4 mg, 3.8 x 10^{-6} mol) were dissolved in 4 ml of DMF and stirred together at 40 °C overnight. To this solution, 8 ml of H_2O were added drop wise over 20 h. The final solution was dialysed against water for 3 h and freeze dried.

Cell culture. The A2780 cell lines were grown in a ventilated tissue culture flask T-75 using Roswell Park Memorial Institute (RPMI-1640) media containing 10% Foetal Bovine Serum (FBS) and antibiotics. The cells were incubated at 37 °C under a 5% CO_2 humidified atmosphere and passaged every 2–3 days when monolayers at around 80% confluence were formed. The cell

View Article Online
DOI: 10.1039/C5TB02429C

density was determined by counting the number of viable cells using a trypan blue dye (Sigma-Aldrich) exclusion test.

Cell viability. The cytotoxicity of the pro-drug, the polymer and the micelles loaded with pro-drug was measured by a standard sulforhodamine B colorimetric proliferation assay (SRB assay). The SRB assay was established by the U.S. National Cancer Institute for rapid, sensitive, and inexpensive screening of antitumor drugs in microtiter plates. The cells were seeded at a density of 5000 cells per well in 96-well plates containing 200 µL of growth medium per well and incubated for 24 h. The medium was then replaced with fresh medium (200 µL) containing various concentrations of the material being tested.

After 48 h incubation, cells were fixed with trichloroacetic acid 10% w/v (TCA) before washing, incubated at 4 °C for 1 h, and then washed five times with tap water to remove TCA, growth medium, and low molecular weight metabolites. Plates were air dried and then stored until use. TCA-fixed cells were stained for 30 min with 0.4% (w/v) SRB dissolved in 1% acetic acid. At the end of the staining period, SRB was removed and cultures were quickly rinsed five times with 1% acetic acid to remove the unbound dye. Then the cultures were air dried until no conspicuous moisture was visible. The bound dye was shaken for 10 min. The absorbance at 570 nm of each well was measured using a microtiter plate reader scanning spectrophotometer BioTek's PowerWave™ HT Microplate Reader and the KC4™ Software. All experiments were repeated three times.

Dose–response curves were plotted (values were expressed as the percentage of control, medium only) and IC50 inhibitory concentrations were obtained using the software Graph Pad PRISM 6.

$$\text{Cell viability (\%)} = (OD_{490,sample} - OD_{490,blank}) / (OD_{490,control} - OD_{490,blank}) \times 100$$

Cellular Uptake. Cellular uptake experiments were performed according to a previously described method with some modifications[40] A2780 cells were seeded into a 6-well plate at 1×10^5 cells per well and incubated until a confluence of 70-80% is reached. The cells were treated with CA-Pt loaded nanoparticles and CA-Pt alone with equal Pt concentrations. After 3 h incubation at 37 °C, the medium was removed and rinsed with cold PBS (3 mL × 3). The cells were trypsinized and incubated with HNO_3 (68%, v/v) at 65 °C for 20 h. Platinum content uptake was determined using inductively coupled plasma mass spectrometer (ICP-MS).

Analysis

Nuclear magnetic resonance (NMR) spectroscopy. ^{1}H NMR spectra were recorded using a Bruker DPX (300 MHz) spectrometer, using D_2O and d_6-DMSO as the solvent. All chemical shifts are stated in ppm (δ) relative to tetramethylsilane (δ = 0 ppm), referenced to the chemical shifts of residual solvent resonances.^{195}Pt NMR spectra were recorded using a Bruker AVANCE III 400 MHz spectrometer, using d_6-DMSO as solvent. The ^{195}Pt NMR spectra have been calibrated using a K_2PtCl_4 standard in D_2O. [^{1}H-^{13}C] HSQC NMR, [^{1}H-^{13}C] HMBC NMR, [^{1}H-^{13}C] COSY NMR and J resolved experiments were recorded using Bruker 500 MHz and Bruker AVANCE III HD 600 MHz as indicated.

Dynamic light scattering (DLS). The average hydrodynamic diameters and size distribution of the prepared micelle solution in an aqueous media at a concentration of 1 mg mL^{-1} were obtained using the Malvern Nano-ZS as a particle size analyzer (laser, 4 mW, λ = 632 nm; measurement angle 12.8° and 175°). Samples were filtered to remove dust using a microfilter 0.45 µm prior to the measurements and run at least three times at 25 °C.

Transmission electron microscopy (TEM). The TEM micrographs were obtained using a JEOL 1400 transmission electron microscope. The instrument operates at an accelerating voltage of 100 kV. The samples were prepared by casting the micellar solution (1 mg mL^{-1}) onto a formvar-coated copper grid. Phosphotungstic acid (PTA) staining was employed.

Thermogravimetric analysis (TGA). TGA studies were carried out under an air atmosphere and the heating rate was fixed at 5 °C min^{-1} on a thermal analyser TGA 2950HR V5.4A. The temperature profile for analysis ranged between 50 and 1000 °C with a five minute isothermal condition at 100 °C. The mass of the samples used in this study was 10 mg.

Inductively Coupled Plasma–Mass Spectrometer (ICP-MS). The Perkin-Elmer ELAN 6000 inductively coupled plasma–mass spectrometer (Perkin-Elmer, Norwalk, CT, U.S.A.) was used for quantitative determinations of platinum. All experiments were carried out at an incident ratio frequency power of 1200 W. The plasma argon gas flow of 12 L min^{-1} with an auxiliary argon flow of 0.8 L min^{-1} was used in all cases. The nebulizer gas flow was adjusted to maximize ion intensity at 0.93 L min^{-1}, as indicated by the mass flow controller. The element/mass detected was ^{195}Pt and the internal standard used was ^{193}Ir. Replicate time was set to 900 ms and the dwell time to 300 ms. Peak hopping was the scanning mode employed and the number of sweeps/readings was set to 3. A total of 4 replicates were measured at a normal resolution. The samples were treated with aqua regia solution at 90 °C for 2 h to digest platinum.

Results and discussion

The block copolymer was obtained via RAFT polymerization using CPADB as chain transfer agent (CTA) and AIBN as initiator.[41] Firstly, OEGMEMA was polymerised generating the macro-CTA agent and the hydrophilic block. A ratio of [OEGMEMA]/[CPADB]/[AIBN] = 60:1:0.1 was used and the polymerization was carried out at 60 °C. The conversion monomer/polymer was calculated from the ^{1}H NMR of the crude solution and the dispersity was determined via GPC analysis. After 12 h polymerization 66% conversion was obtained resulting in a POEGMEMA macro-CTA of 40 units, M_n = 13800 g mol^{-1} and $Đ$ = 1.1 (Fig. 1).

The TMSPMA monomer was synthesised via coupling reaction between 3-(trimethylsilyl) propargyl alcohol and methacryloyl chloride. The choice of this monomer hails from the presence of the

View Article Online
DOI: 10.1039/C5TB02429C

triple bond which, once deprotected, can be easily clicked with an azide functionality.[42] The trimethylsilyl protecting group was deemed necessary to avoid unnecessary side reactions during the polymerization. POEGMEMA was then chain extended with TMSPMA using a ratio of [POEGMEMA]/[TMSPMA]/[AIBN] = 1:100:0.1. A 12 h polymerization at 60 °C gave 60% conversion, 60 units of TMSPMA and a block copolymer with M_n = 23800 g mol^{-1} and $Đ$ = 1.20 (Fig. 1 and Fig. 2 a). The alkyne groups of the block copolymer were deprotected using acidic conditions. ^{1}H NMR confirmed that the reaction was successful and the block copolymer was fully deprotected. The sharp peak at 0.15 ppm of the trimethylsilyl disappears completely whilst the alkyne functionality appears at 2.55 ppm (Fig. 2 b). During this process the RAFT endfunctionality is lost and replaced by the hydrogen, which has been shown in an earlier study using Electrospray Ionisation Mass Spectrometry.[43] A small fraction of RAFT functionality has been converted to a double bond as a result of the Chugaev reaction as evidenced by the vinyl signals in the area of 5.5 and 6 ppm.[44] The GPC analysis showed a reduction of the molecular weight to M_n = 20000 g mol^{-1} and a similar dispersity to the polymer before deprotection (Fig. 1).

β-CD was modified in 6-position with the azide group through tosylation. Mono-6-(p-toluenesulfonyl)-β-cyclodextrin was prepared from β-CD and p-toluenesulfonyl chloride. The toluenesulfonyl leaving group was then replaced by the azide group by reaction with NaN_3 (Fig. 2 c). The so functionalised β-CD (N_3- β-CD) was then grafted onto the block copolymer by copper(I)-catalyzed azide–alkyne cycloaddition (click-reaction).[45, 46] The catalyst was removed using a copper chelating resin. In fact, precipitation or dialysis purification methods were not found sufficient to fully remove the catalyst. The unreacted CD was removed via dialysis against DMSO followed by dialysis against water. Analysis by ^{1}H NMR confirmed that 80% of the propargyl functionality was converted to CD (Fig. 1 and Fig. 2 d). The measured molecular weight was found to be in good agreement with the expected value although the final product has a rather broad distribution, which is in good agreement with other reports that highlight the encountered similar difficulties.

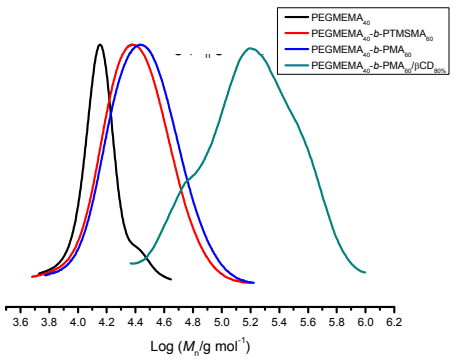

Figure 1: GPC analysis in DMAc of $POEGMEMA_{40}$ (black), $POEGMEMA_{40}$-*b*-$PTMSPMA_{60}$ (red), after deprotection $POEGMEMAA_{40}$-*b*-PMA_{60} (blue) and after βCD grafting $POEGMEMA_{40}$-*b*-PMA_{60}-*g*-βCD.

Table 1. Molecular weight measured by GPC and compared to the theoretical value

Polymer	M_n/ g mol^{-1} (GPC)	Đ	M_n/ g mol^{-1} (theo)
$POEGMEMA_{40}$	13800	1.11	12000
$POEGMEMA_{40}$-*b*-$TMSPMA_{60}$	23800	1.20	23760
$POEGMEMA_{40}$-*b*-PMA_{60}	20000	1.28	19440
$POEGMEMA_{40}$-*b*-PMA_{60}-*g*-βCD	96000	1.70	74016

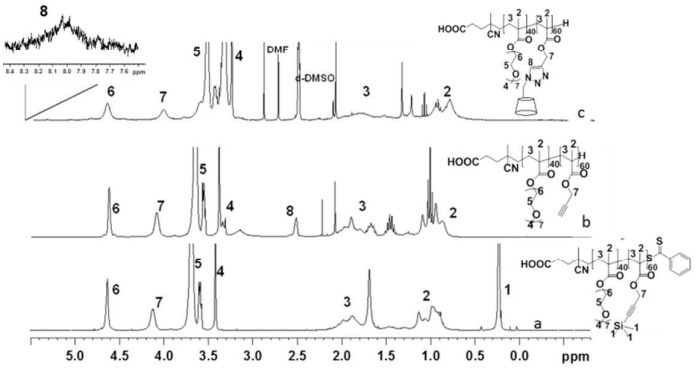

Figure 2: ^{1}H-NMR analysis of a) POEGMEMA-*b*-TMSPMA ($CDCl_3$); b) after deprotection POEGMEMA-*b*-PMA ($CDCl_3$); c) $POEGMEMA_{40}$-*b*-PMA_{60}-*g*-βCD (d_6-DMSO)

Synthesis and NMR characterization of the platinum pro-drug

Cholic acid (CA) is a primary bile acid insoluble in water. It has been previously reported that cholic acid interacts with β-CD[47] forming an inclusion complex. Moreover, the carboxylic group present in the cholic acid structure can be used as conjugation site in the reaction with oxoplatin. Oxoplatin was prepared by oxidation of the commercially used cisplatin and then coupled with the cholic acid so forming the Pt(IV) pro-drug CA-Pt. Oxoplatin was used in slight excess compared to cholic acid in respect to the two hydroxo groups available (1:1.9 ratio oxoplatin/cholic acid) to avoid an excess of unreacted cholic acid which would be difficult to separate from CA-Pt. ^{195}Pt NMR (Fig. 3) confirmed the success of the coupling reaction. The peak at 1047 ppm corresponds to the mono-substituted specie whilst the peak at 1227 ppm corresponds to the di-substituted specie. Considering the 1:0.7 ratio between the areas of the two peaks we estimate that di-substituted specie represent the 70% of the mixture whilst the mono-substituted specie abundance is 30%. The low solubility of the resulting product in most solvents does not allow the separation of the products using chromatography methods.

View Article Online
DOI: 10.1039/C5TB02429C

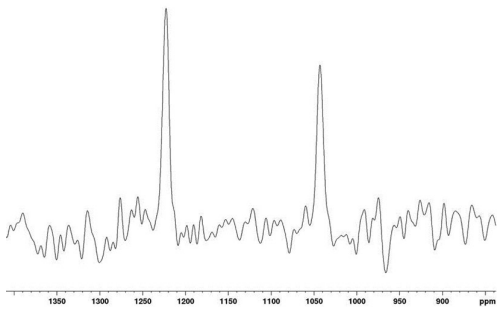

Figure 3. 195Pt NMR, d6-DMSO. The spectrum has been calibrated using a K_2PtCl_4 standard

The crosslinker CA-Pt was further characterized via NMR analysis. A range of 2D spectra were recorded (COSY, NOESY, [^{1}H-^{13}C] HSQC, TOCSY and ROESY NMR (ESI, Figure S2 – S6)) together with the J resolved experiments to be able to identify all ^{1}H-NMR signals and confirm the structure of the drug. The assigned signals are listed in the ESI is a tabulated manner (ESI, Table S7).

Host-guest interaction

The main object of this project was to study the affinity between a host such as β-CD and a platinum based pro-drug. In fact, it is well known that the interaction between β-cyclodextrin and a hydrophobic molecule will drastically increase the solubility of the latter. To prepare the β-CD/CA-Pt complex two solutions were prepared: β-CD is dissolved in distilled water whilst CA-Pt is dissolved in THF. The THF solution is added slowly to the water solution under fast stirring until the mixture turns turbid obtaining a mixture β-CD/CA-Pt in a ratio of 2:1. The mixture turns clear when heated at 40 °C. The slow evaporation of THF will force the hydrophobic CA-Pt to interact with the β-CD to remain in the water solution. After complete evaporation of THF the water solution was observed to be clear with no CA-Pt precipitated. Subsequent freeze drying yields a colourless powder that can be easily redissolved in water. The complex formation was investigated using NMR. Fig. 4 displays the ^{1}H NMR of β-CD and CA-Pt alone (a and c respectively) and β-CD/CA-Pt (b). A major change in chemical shift can be noticed for the proton H_5 of the CD (Fig. 4, b and c) The shift of H_5 towards higher fields (Δδ = 0.1) is typical of host-guests CD complexes.[48, 49]

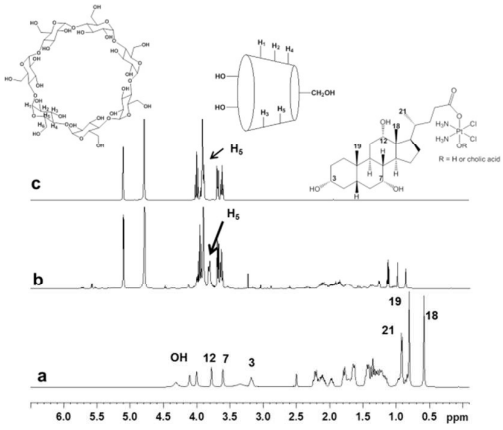

Figure 4. ^{1}H NMR, 500 MHz, a) CA-Pt in d_6-DMSO, b) β-CD/CA-Pt in D_2O, c) β-CD in D_2O

All observed shifts Δδ, which are the result of the interaction of CA-Pt with β-CD are summarised in table (S8). Moreover, 2D NMR experiments (Supporting Info (S9 – S11)) aid the identification of the interactions. Small changes in chemical shifts (Δδ ≤ 0.2 ppm) can be justified by the different deuterated solvent used for the measurement: D_2O in the case of β-CD/CA-Pt and d-DMSO in the case of CA-Pt. A major shift towards lower fields of the three methyl groups (18, 19, 21) was noticed whilst the three hydroxyl groups are no longer visible in spectrum b due to the exchange of the proton with deuterium from D_2O (Fig. 4, a and b). To further confirm that the CA-Pt chemical shifts are not only caused by different deuterated solvents used but by the presence of the cyclodextrin in the solution ^{1}H NMR of the CA-Pt in D_2O was recorded. Due to the high hydrophobicity of the CA-Pt only a very low concentration solution can be prepared resulting in poor resolution of most of the peaks. However peaks 18, 19 and 21 are still sufficiently allowing to compare the chemical shifts of peak 18, 19 and 21 in the three different conditions (Figure 5). The resonances move to lower fields when using D_2O instead of d_6-DMSO. However, a further shift towards lower fields can be noticed in the presence of CD. Generally, the shift towards lower fields is due to decreased shielding of the electrons. In fact, d_6-DMSO (Fig. 5, a) solvates well the three methyl groups causing high shielding of the electrons. Conversely, D_2O does not solve them very well leading to a lower shielding of the electrons and so a shift of the peaks to lower fields. Lastly, once the cholic acid moiety of CA-Pt is encapsulated by the CD (Fig. 5, c) the solvent around it is pushed away lowering even more the shielding thus shifting the peaks to even lower fields.

View Article Online
DOI: 10.1039/C5TB02429C

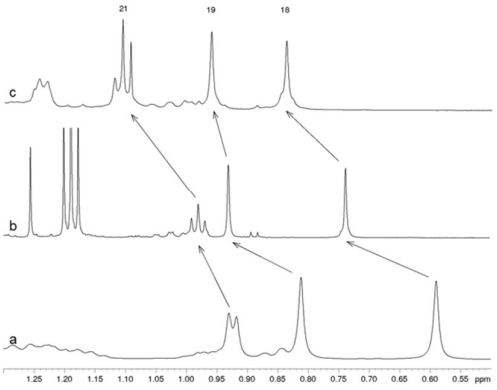

Figure 5. **a)** ^{1}H NMR, 500 MHz, CA-Pt in d_6-DMSO **b)** ^{1}H NMR, 600 MHz, CA-Pt in D_2O, **c)** β-CD/CA-Pt in D_2O

Moreover, Figure 6 depicts the overlap of [^{1}H-^{13}C] HSQC of CA-Pt and the complex. It is evident that peaks 3, 7 and 12 shifts towards lower fields in presence of the CD.

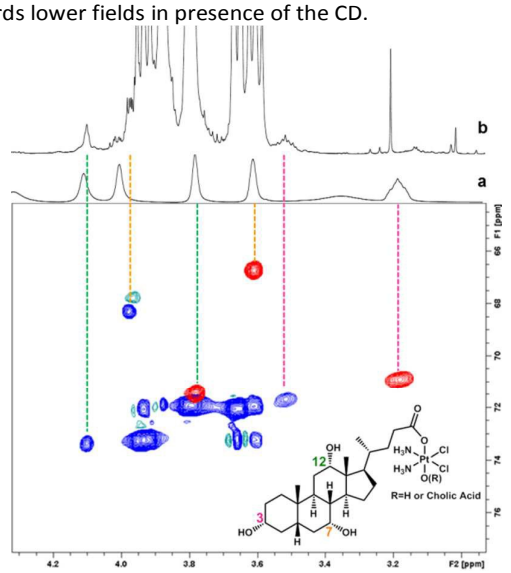

Figure 6. (red) [^{1}H-^{13}C] HSQC, 500 MHz, CA-Pt in d-DMSO; **a** ^{1}H NMR, 500 MHz, CA-Pt in d_6-DMSO; (blue) [^{1}H-^{13}C] HSQC, 500 MHz, β-CD/CA-Pt in D_2O; **b** ^{1}H NMR, 500 MHz, β-CD/CA-Pt in D_2O

Further evidence of the occurring complexation was obtained by measuring the diffusion coefficients of β-CD, CA-Pt and complex in two different environments, D_2O and d-DMSO. The diffusion parameters have been measured using DOSY NMR experiment. Results are summarized in Table 2. As expected, β-CD diffuses with a slower rate in d_6-DMSO than D_2O due to the higher viscosity of DMSO whilst CA-Pt diffuses in d_6-DMSO similarly to β-CD. The first indication of interaction between β-CD and CA-Pt is given by the presence of a single chemical shift which indicates that the two molecules diffuse at the same rate. Moreover, the complex has a diffusion coefficient slightly lower than the β-CD alone indicating, as expected, a slight bigger volume of the complex compare to the β-CD alone.

Table 2. Diffusion parameter and diffusion coefficient obtained from DOSY experiments of β-CD, CA-Pt and complex β-CD/CA-Pt in D2O and d6-DMSO.

	Solvent	Diffusion parameter [log(m^2/s)]	Diffusion coefficient [m^2/s]
β-CD	D_2O	-9.31	4.89 x 10^{-10}
β-CD	d_6-DMSO	-9.68	2.09 x 10^{-10}
CA-Pt	d_6-DMSO	-9.60	2.51 x 10^{-10}
β-CD/CA-Pt	D_2O	-9.25	4.36 x 10^{-10}

Micelles preparation and their characterization

The block copolymer dissolves directly in water. It does not show any obvious amphiphilic features and thus is not able to self-assemble in aqueous media as evidenced by the absence of typical nanoparticles as measured using DLS. The PEGMEMA side chain could have potentially interacted with β-CD as seen in earlier work,[20] but aggregate formation was absent this time. It also needs to be considered that α-cyclodextrin is more suitable for the inclusion complex formation with PEO.[50] Within the concentration range measured, (c < 1 mg ml^{-1}) the scattering intensity changes linearly with conversion, indicative of the absence of any aggregate formation in this range (Fig. 7). However, the interaction between CA-Pt and β-CD grafted onto the polymer introduces hydrophobicity to the CD block enabling the formation of micelles. Micelles were prepared by dissolving both, block copolymer and pro-drug, in DMF at a ratio of 2:1 of grafted β-CD to CA-Pt. The mixture was stirred overnight at 40 °C. Addition of H_2O to this solution pushes the hydrophobic pro-drug towards the hydrophobic cavity of the cyclodextrins giving the block copolymer a more pronounced amphiphilicity triggering the formation of nanoparticles. The resulting solution does not show the presence of any precipitate suggesting that all water-insoluble CA-Pt is safely encapsulated in the CD cavity. The nanoparticles were imaged with TEM after dialysis using PTA staining revealing spherical nanoparticles with diameters of 200 nm (Fig. 8), which is in agreement with the DLS results (Fig.11). It should be noted here that considering the block lengths of the block copolymers the resulting nanoparticles are less likely to be well-defined core-shell micelles, but rather large-compound micelles. Possible reason may be the rate of water addition to the polymer/drug mixture in organic solvent. Water pushes the drug inside the CD cavity, but also enables the self-assembly. Although the water addition was carried out over one day here, it might have still been too fast to enable the formation of well-defined micelles.

View Article Online
DOI: 10.1039/C5TB02429C

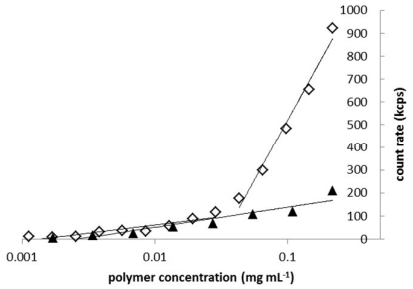

Figure 7: Scattering intensity *vs* the concentration of CA-Pt loaded POEGMEMA$_{40}$-*b*-PMA$_{60}$-*g*-βCD NPs (◇) and POEGMEMA$_{40}$-*b*-PMA$_{60}$-*g*-βCD (▲) in water.

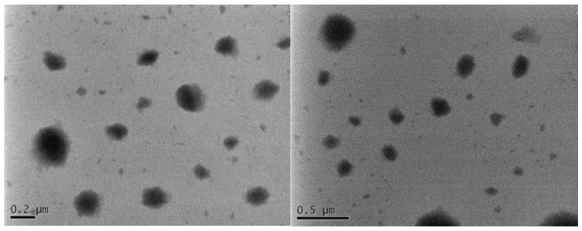

Figure 8. TEM analysis of CA-Pt loaded POEGMEMA$_{40}$-*b*-PMA$_{60}$-*g*-βCD

The content of platinum pro-drug into the micelles was measured via thermogravimetric Analysis. The platinum content of 4.5% equals to 93% of the drug being loaded into the micelles. The high loading efficiency indicates that only a negligible amount of drug was lost during dialysis and can be seen as a measure of the high stability of the CD-cholic acid complex in deionized water. The stability of the micelles upon dilution was investigated using DLS. Determining the CAC concentration is not only necessary to confirm the induced amphiphilicity compared to the unloaded POEGMEMA$_{40}$-*b*-PMA$_{60}$-*g*-βCD, but also to evaluate the stability in a delivery scenario. The scattering intensity was recorded at a fixed aperture, which revealed that a critical aggregate concentration of $2.8 \times 10^{-2} \pm 0.5 \times 10^{-2}$ mg ml^{-1}.

Proton NMR of the grafted polymer was measured before and after the formation of micelles. With the formation of micelles the relaxation time of the core-forming block changed which is evident by the suppressed signal intensity.[51] Using the POEGMEMA signals as internal standard, the intensity of cyclodextrin moieties drastically decreases when the polymer is loaded with pro-drug and assembled into micelles. Furthermore, the cyclodextrins peaks appear broad and poorly resolved in the micellar state suggesting that the cyclodextrin moieties are in the core of the micelles while simultaneously entrapping the drug.

The host-guest interaction between the drug and CD induced amphiphilic features to the polymer providing protection to the otherwise in water insoluble drug. At this point, it can only be assumed that the drug also acts as crosslinker since pendant cholic acid would seek out the hydrophobic CD cavity, a process which is supported by the 1:1 ratio between CD and the cholic acid functionality. Further evidence for the presence of crosslinks is the strong interaction between bile acid and cyclodextrin,[35, 52] which has been used earlier to generate self-healing hydrogels.[53]

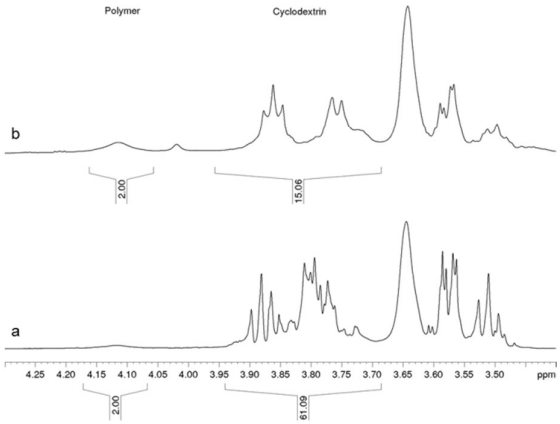

Figure 9: ^{1}H NMR, 600 MHz, **a)** POEGMEMA$_{40}$-*b*-PMA$_{60}$-*g*-βCD in D_2O; **b)** drug loaded micelles in D_2O

The release of the drug in deionized water was found to be negligible as evidence by the high loading capacity after purification *via* dialysis. The release of the platinum drug can be triggered in a reductive environment such as the intracellular environment, which was simulated here by the addition of ascorbic acid of ascorbic acid (5 mM). Under these conditions the Pt(IV) drug is reduced to Pt(II), which will be released from the nanoparticles (Figure 10). Since the system is stable in water, it is reasonable to assume that the drug can only be released *via* reduction. The micelle solution was dialysed at 37 °C using a membrane (MWCO 3500). Samples were taken from inside of the membrane at regular intervals. ICP-MS was used to monitor the amount of platinum released. As shown in Figure 10 about 70% of the drug is gradually released over 24 hours. Direct analysis of the released species is difficult as the released Pt(II) drug will form various complexes with water and ascorbic acid. An initial burst of drug from a delivery system is typical, in particular when the drug is physically encapsulated. For polymer-drug conjugated systems this can be avoided by stabilizing the system by crosslinking. In our delivery system, the pro-drug acts as a crosslinker stabilizing the PEGMEMA-b-PMA-g-βCD micelles. Furthermore, we hypostasize that the release of platinum occurs upon cleavage of the cholic acids moieties which keep their interaction with the CDs. Thus, the slow release is due to the fact that a reduction reaction has to take place for the platinum to be release.

View Article Online
DOI: 10.1039/C5TB02429C

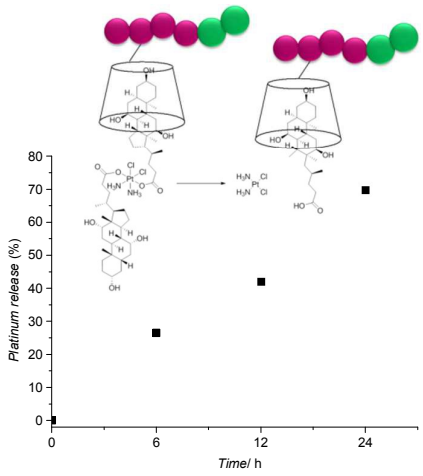

Figure 10: Release of platinum drug as cisplatin in the presence of ascorbic acid (5 mM)

The micelles formation and disassembly after the release of the pro-drug was investigated via DLS (Fig. 11). The polymer in water has a diameter of D_h = 19 ± 0.33 nm. After self-assembly, the micelles have a diameter of D_h = 266 ± 0.48 nm which is maintained after lyophilisation and redispersion in water. After the release of cisplatin in presence of ascorbic acid the volume decreases again to D_h = 65 ± 0.38 nm. This indicates that bile acid largely remains in the CD cavity after the release of the platinum drug helping to maintain the amphiphilicity. Furthermore, the possibility that cisplatin may have been recaptured by empty CD cavities was entertained. However, intensive NMR studies showed that there is no evidence that cisplatin is a stable guest molecules in β-CD.

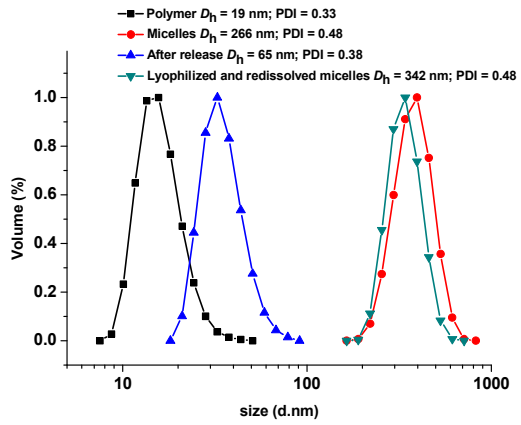

Figure 11: DLS curves of the grafted polymer (black); micelles (red); lyophilized and redissolved micelles (green); after release (blue).

Biological evaluation

The cytotoxicity of the block copolymer was assessed by SRB assay. Proliferation of platinum resistant ovarian cancer cell line A2780 was investigated at different concentrations of the block copolymer. Even at a high concentration of 75 mg mL^{-1}, the polymer was not found to inhibit cell proliferation, as compared to cells exposed to normal growth conditions (Fig. 12, a). Therefore, the toxicity resulting from the synthetic procedure could be excluded. Due to its high hydrophobicity, the cytotoxicity of CA-Pt was investigated upon encapsulation into Me-β-CD. Unlike β-CD, Me-β-CD is known to be non-toxic on its own so it will not interfere with the toxicity of CA-Pt. β-CD, instead, results to be toxic if administrated to cells but it loses toxicity when part of a polymer carrier. On A2780 cells, Me-β-CD/CA-Pt shows an IC_{50} = 34.7 μM (Fig. 12, b). Subsequently, the drug loaded nanoparticle was studied. The polymer concentrations employed in this *in vitro* study ranged from 11 mg ml^{-1} to 4.3 x 10^{-2} mg ml^{-1} and lies therefore above the measured CAC concentration, which is a crucial consideration since disassembled block copolymers were shown to have a low cellular uptake only.[54] The IC_{50} value of the drug delivered with the nanoparticle nearly halves compared to the free drug loaded into Me-β-CD (IC_{50} = 20.4 μM) (Fig. 12, c).[55]

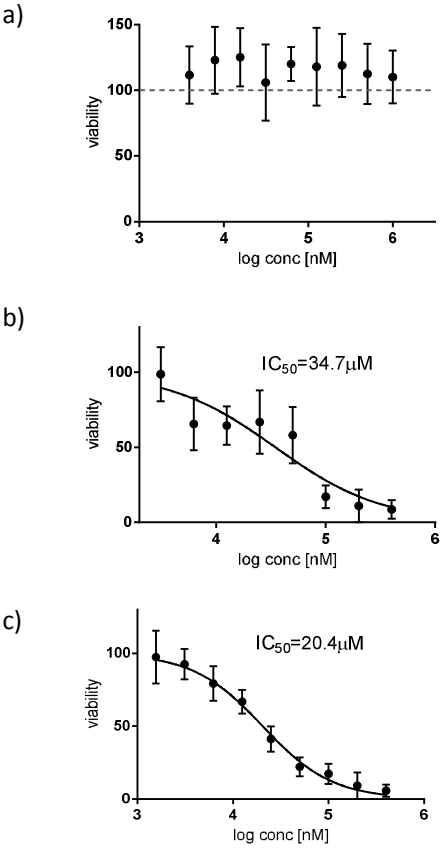

Figure 12: Cytotoxicity assays on A2780 of **a)** polymer carrier, **b)** Me-β-CD/CA-Pt, **c)** CA-Pt loaded micelles

It is hypothesized that the higher toxicity stems from the more efficient cellular uptake when delivered in a nanocarrier. To investigate the uptake of platinum into cells, A2780 were

View Article Online
DOI: 10.1039/C5TB02429C

seeded into 6-well plates and grown up to a confluence of 70-80%. The cells were then loaded with Me-β-CD/CA-Pt or CA-Pt loaded nanoparticles at a concentration of 50 μM of platinum and incubated for 3 h at 37 °C. The cells were then washed three times with PBS to remove free Me-β-CD/CA-Pt or CA-Pt loaded NPs, trypsinised and collected for digestion. The digested solutions were analysed *via* ICP-MS to determine the platinum content. The difference in platinum content inside the cells is depicted in Fig. 13. The significantly higher uptake of platinum when encapsulated into the micelles may be one of the factors contributing to the lower IC_{50} value of the nanoparticles.

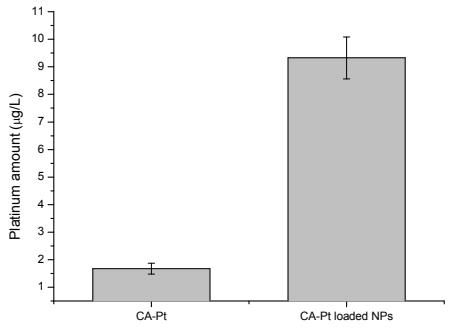

Figure 13: Uptake analysis of CA-Pt and CA-Pt loaded NPs on A2780

Conclusion

With a combination of RAFT-polymerization and chick chemistry we have successfully prepared an amphiphilic block copolymer with pendant β-cyclodextrins able to physically encapsulate a Pt(IV) pro-drug. We have modified the commercially available cisplatin firstly via oxidation and later via coupling reaction with cholic acid. The Pt(IV) pro-drug interacts with the pendant β-cyclodextrins driving the formation of micelles where CA-Pt is entrapped. We have tested the bio-activity of the CA-Pt loaded micelles and compared to the CA-Pt alone. Cytotoxicity assays on ovarian cancer cell line A2780 have proved the non-toxicity of the polymer carrier. Moreover, the encapsulation of CA-Pt into micelles drastically improves the cytotoxicity profile. The lower IC_{50} value showed by the micelles compare to the drug alone can be explained by the higher uptake. In fact, ICP-MS measurement have proved that cells treated with CA-Pt loaded micelles contain about 6 fold the amount of platinum.

Acknowledgements

The authors like to thank the Australian Research Council (ARC DP1092694) for funding.

Notes and references

1. J. Reedijk, *Eur JIC*, 2009, **2009**, 1303-1312.
2. L. Kelland, *Nat Rev Cancer*, 2007, **7**, 573-584.
3. L. Kelland, *Expert Opin. Investing. Drug*, 2007, **16**, 1009-1021.
4. V. T. Huynh, W. Scarano and M. H. Stenzel, in *Nanopharmaceutics*, pp. 201-241.
5. M. Callari, Aldrich-Wright, J. R., de Souza, Paul L., Stenzel, M. H., *Progr. Polym. Sci.*, 2014, **39**, 1614-1643.
6. S. Bisht, Maitra, A., *Wiley Interdiscip Rev Nanomed Nanobiotechnol.*, 2009, **1**, 415-425.
7. I. H. L. Hamelers and A. I. P. M. de Kroon, *J. Liposome Res.*, 2007, **17**, 183-189.
8. A. I. P. M. de Kroon, R. W. H. M. Staffhorst, B. de Kruijff and K. N. J. Burger, *Methods in Enzymology* 2005, **391**, 118-125.
9. L. L. Komane, Mukaya, E. H., Neuse, E. W., van Rensburg, C. E. J., *JIOPM*, 2007, **18**, 111-123.
10. I. Rosenbaum, Harnoy, A. J., Tirosh, E., Buzhor, M., Segal, M., Frid, L., Shaharabani, R., Avinery, R., Beck, R., Amir, R. J., *J. Am. Chem. Soc.*, 2015, **137**, 2276-2284.
11. B. Schlechter, Neumann, A., Wilchek, M., Arnon, R., *J. Controlled Release*, 1989, **10**, 75-87.
12. C. B. dos Santos, M. P. Mazzobre, M. F., *J Sci Food Agric*, 2011, **91**, 2551-2557.
13. V. Cucinotta, Mangano, A., Nobile, G., Santoro, A. M., and Vecchio G., *J Inorg Biochem*, 1993, **52**, 183-190.
14. M. X. Zhao, Zhao, M., Zeng, E. Z., Li, Y., Li, J. M., Cao, Q., Tan, C. P., Ji, L. N., Mao, Z. W., *J Inorg Biochem*, 2014, **137**, 31-39.
15. A. M. Krause-Heuer, N. J. Wheate, M. J. Tilby, D. G. Pearson, C. J. Ottley and J. R. Aldrich-Wright, *Inorg Chem*, 2008, **47**, 6880-6888.
16. Y. Shi, Goodisman, J., Dabrowiak, J. C., *Inorg Chem*, 2013, **52**, 9418-9426.
17. D. Prashar, Shi, Y., Bandyopadhyay, D., Dabrowiak, J. C., Luk, Y. Y., *Bioorg Med Chem Lett*, 2011, **21**, 7421-7425.
18. J. Zhou and H. Ritter, *Polym. Chem.*, 2010, **1**, 1552-1559.
19. B. V. K. J. Schmidt, M. Hetzer, H. Ritter and C. Barner-Kowollik, *Progr. Polym. Sci.*, 2014, **39**, 235-249.
20. F. Yhaya, J. Lim, Y. Kim, M. Liang, A. M. Gregory and M. H. Stenzel, *Macromolecules*, 2011, **44**, 8433-8445.
21. Z. Ling, Stenzel M. H., *Aust. J. Chem*, 2009, **62**, 813-822.
22. B. V. K. J. Schmidt and C. Barner-Kowollik, *Polym. Chem.*, 2014, **5**, 2461-2472.
23. R. Machín, Isasi, J. R., Vélaz, I., *Carbohydrate Polymers*, 2012, **87**, 2024-2030.
24. A. Harada, Y. Takashima and M. Nakahata, *Accounts of Chemical Research*, 2014, **47**, 2128-2140.
25. Z. Fülöp, S. V. Kurkov, T. T. Nielsen, K. L. Larsen and T. Loftsson, *J. Drug Delivery Sci. Tech.*, 2012, **22**, 215-221.
26. J. Zhang and P. X. Ma, *Adv. Drug Delivery Rev.*, 2013, **65**, 1215-1233.
27. F. Yhaya, S. Binauld, Y. Kim and M. H. Stenzel, *Macromolecular Rapid Communications*, 2012, **33**, 1868-1874.
28. Y. Kim, Binauld, S., Stenzel, M. H., *Biomacromolecules*, 2012, **13**, 3418-3426.
29. J. Fang, H. Nakamura and H. Maeda, *Adv. Drug Delivery Rev.*, 2011, **63**, 136-151.
30. J. Fang, Sawa, T., Maeda, H., in *Polymer Drugs in the Clinical Stage*, Springer US, 2003, pp. 29-49.
31. J. Eliezar, Scarano, W., Boase, N. R. B., Thurecht, K. J., Stenzel, M. H., *Biomacromolecules*, 2015, **16**, 515-523.
32. D. E. Owens, Peppas, N. A., *Inter. J. Pharm.*, 2006, **307**, 93-102.
33. A. Matsumoto, Matsukawa, Y., Suzuki, T., Yoshino, H., *J Control Release*, 2005, **106**, 172-180.
34. Y. Xue, Tang, X., Huang, J., Zhang, X., Yu, J., Zhang, Y., Gui, S., *Colloids Surf B Biointerfaces*, 2011, **85**, 280-288.
35. Z. J. Tan, X. X. Zhu and G. R. Brown, *Langmuir*, 1994, **10**, 1034-1039.

View Article Online
DOI: 10.1039/C5TB02429C

36. M. Baptissart, Vega, A., Maqdasy, S., Caira, F., Baron, S., Lobaccaro, J.-M. A., Volle, D. H., *Biochimie*, 2013, **95**, 504-517.
37. S. Oae, Okabe, T., Yagihara, T., *Tetrahedron*, 1972, **28**, 3203-&.
38. Y. Mitsukami, M. S. Donovan, A. B. Lowe and C. L. McCormick, *Macromolecules*, 2001, **34**, 2248-2256.
39. A. R. Khan, P. Forgo, K. J. Stine and V. T. D'Souza, *Chem Rev*, 1998, **98**, 1977-1996.
40. R. Xinga, Wang X., Zhanga, C., Zhanga, Y., Wanga, Q., Yanga, Z., Guoa, Z. , *J Inorg Biochem*, 2009, **103**, 1039-1044.
41. A. Gregory and M. H. Stenzel, *Progr. Polym. Sci.*, 2012, **37**, 38-105.
42. A. B. J. Withey, Chen, G., Nguyen, T. L. Uyen, Stenzel, M. H., *Biomacromolecules*, 2009, **10**, 3215-3226.
43. D. Quemener, M. Le Hellaye, C. Bissett, T. P. Davis, C. Barner-Kowollik and M. H. Stenzel, *J. Polym. Sci. Part a-Polym. Chem.*, 2008, **46**, 155-173.
44. F. Yhaya, S. Binauld, M. Callari and M. H. Stenzel, *Australian Journal of Chemistry*, 2012, **65**, 1095-1103.
45. A. Maciollek, H. Ritter and R. Beckert, *Beilstein J. Organic Chem.*, 2013, **9**, 827-831.
46. S. Amajjahe, S. Choi, M. Munteanu and H. Ritter, *Angew. Chem., Int. Ed.*, 2008, **47**, 3435-3437.
47. O. P. Comini S., Riottot M, Duhamel D, *Clin Chim Acta*, 1994 **228**, 181-194.
48. P. Sompornpisut, Deechalao, N., Vongsvivut, J., *ScienceAsia*, 2002, **28**, 263-270.
49. F. B. T. Pessine, Calderini, A., Alexandrino, G. L., *Interchopen*, 1998, **1**.
50. A. Harada and M. Kamachi, *Macromolecules*, 1990, **23**, 2821-2823.
51. I. Furó, *J. Molecular Liquids*, 2005, **117**, 117-137.
52. C. Schönbeck, P. Westh, J. C. Madsen, K. L. Larsen, L. W. Städe and R. Holm, *Langmuir*, 2010, **26**, 17949-17957.
53. Y.-G. Jia and X. X. Zhu, *Chem. Mater.*, 2015, **27**, 387-393.
54. Y. Kim, Pourgholami, M. H., Morris, D. L., Stenzel, M. H., *Biomacromolecules*, 2012, **13**, 814-825.
55. E. C. Aimee, Page H. M., M. C. Phillips and R. G. H, *J. Lipid Res.*, 1997, **38**, 2265-2272.

View Article Online
DOI: 10.1039/C5TB02429C